STANFORD RESEARCH INSTITUTE
MENLO PARK, CALIFORNIA

24 p.

[redacted]

June 1964

UNPUBLISHED PRELIMINARY DATA

Quarterly Technical Summary Report No. 3 December 1, 1963 to May 31, 1964

[redacted]

MECHANICAL PROPERTIES OF CROSSLINKED POLY(METHYL METHACRYLATE) POLYMERS UNDER SPACE ENVIRONMENTAL CONDITIONS

Prepared for:

National Aeronautics and Space Administration
Washington 25, D.C.

Contract No. NASr-49(13)

By: N. W. Tschoegl T. L. Smith

SRI Project No. PRU-4520

Approved:

Thor L. Smith

Thor L. Smith, Director
Propulsion Sciences Division

Copy No. 2

[redacted]

REPORTS CONTROL No. _____

ABSTRACT

29459

Tensile stress-strain data were obtained on two samples of poly(methylmethacrylate) (PMMA) crosslinked to differing degrees with glycol dimethacrylate, and on one sample of uncrosslinked PMMA. Plots are shown of the reduced stress vs. time for the uncrosslinked PMMA at different strain values; a failure envelope was obtained from break data on the same material. The concept of the failure envelope, hitherto applied only to crosslinked elastomers, is applicable also to uncrosslinked materials; however, the accessible portion of the failure envelope is reduced because data obtained in stress-strain regions where either yield or flow occurs do not lie on the failure envelope.

The stress relaxometer for continuous and intermittent stress relaxation measurements is described in detail; results in a trial experiment on uncrosslinked PMMA *in vacuo* are presented.

author

[redacted]

CONTENTS

ILLUSTRATIONS

I INTRODUCTION

This third Quarterly Status Report describes work conducted for the National Aeronautics and Space Administration under Task Order NASr-49(13) during the contractual period December 1, 1963, to May 31, 1964. The original period of three months for this report was extended to six months under Amendment No. 1 to Task Order NASr-49(13). The program is monitored by the Ames Research Center of NASA.

The objective of this study of crosslinked poly(methylmethacrylate) (PMMA) polymers is to obtain information on the behavior of crosslinked polymers in space environments. Of particular interest are degradative changes in structure which take place in vacuo at elevated temperatures, the kinetics associated with the degradation process, and the influence of these changes on the mechanical properties of the polymers.

During the reporting period, tensile tests were conducted at various temperatures on two samples of crosslinked PMMA and some further tests were made on uncrosslinked PMMA. The special relaxometer designed for the simultaneous measurements of continuous and intermittent stress relaxation was completed and some test runs were made on commercial PMMA.

II TENSILE STRESS-STRAIN CHARACTERISTICS OF UNCROSSLINKED AND CROSSLINKED PMMA

During the preceding report period tensile tests were conducted in the Instron tester on commercial poly(methylmethacrylate) at ten crosshead speeds at four temperatures above T_g to provide data on an uncrosslinked material so that the results could be compared with those obtained on materials crosslinked to different degrees. In the present report period data were obtained at the same crosshead speeds at four additional temperatures and all data were reduced and analyzed. The temperatures and crosshead speeds ranged from 110 to 165° C, and from 0.02 to 20 inches/minute.

Tensile tests were also conducted at the same eight temperatures and ten crosshead speeds on two crosslinked samples supplied by the Ames Research Center of NASA. These data have not yet been fully reduced.

A. Uncrosslinked PMMA

The methods used in reducing and analyzing the data obtained on the uncrosslinked commercial PMMA differed only in minor details from those developed for amorphous elastomers.[1-4] Values of reduced stress ($273\,\sigma/T$) were first plotted against time in a doubly logarithmic plot for several stretch ratios at each test temperature. (The stretch ratio $\lambda = l/l_0$, where l is the length of the stretched specimen and l_0 is the original length of the specimen.) Empirical shift factors a_T were then obtained by shifting the curves to coincidence along the time axis. The time-temperature superposition factors determined in this way are shown in Fig. 1 in which the solid line represents the universal form of the WLF equation[5]

$$\log a_T = - \frac{8.86(T - T_s)}{101.6 + T - T_s} \quad . \qquad (1)$$

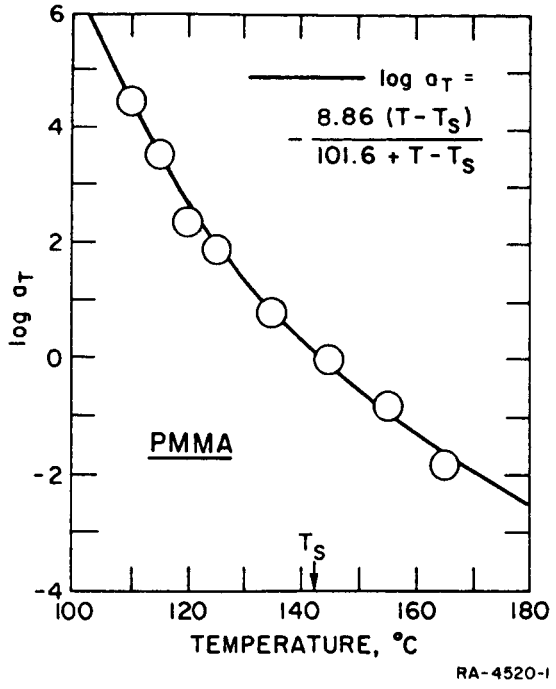

FIG. 1 TEMPERATURE DEPENDENCE OF log a_T FOR UNCROSSLINKED PMMA

This equation predicts a_T for a given temperature T if a characteristic temperature T_s (which is generally about 50 degrees higher than T_g) is known. Conversely, T_s may be determined from empirically obtained a_T values using Eq. (1). This is shown in Fig. 1. The value of T_s obtained in this way (143° C, or 416° K) is very reasonable, although somewhat lower than other values reported for PMMA in the literature.[5]

Shift factors calculated from Eq. (1) with T_s = 143° C were used to make plots of log $\sigma\, T_s/T$ against log t/a_T for a number of stretch ratios. Several of these plots of reduced stress against time are shown in Fig. 2 where A is an arbitrary additive constant used to separate the curves for convenience in presentation. It can be seen that the time-temperature superposition is quite good although there is some scatter in the low temperature data. The 120° C data are everywhere lower than the rest. Figure 1 shows that a_{120} also lies below the WLF-curve. This suggests that the actual test temperature was slightly higher than 120° C. These 120° C data were therefore disregarded in drawing the full curves which represent lines of best fit.

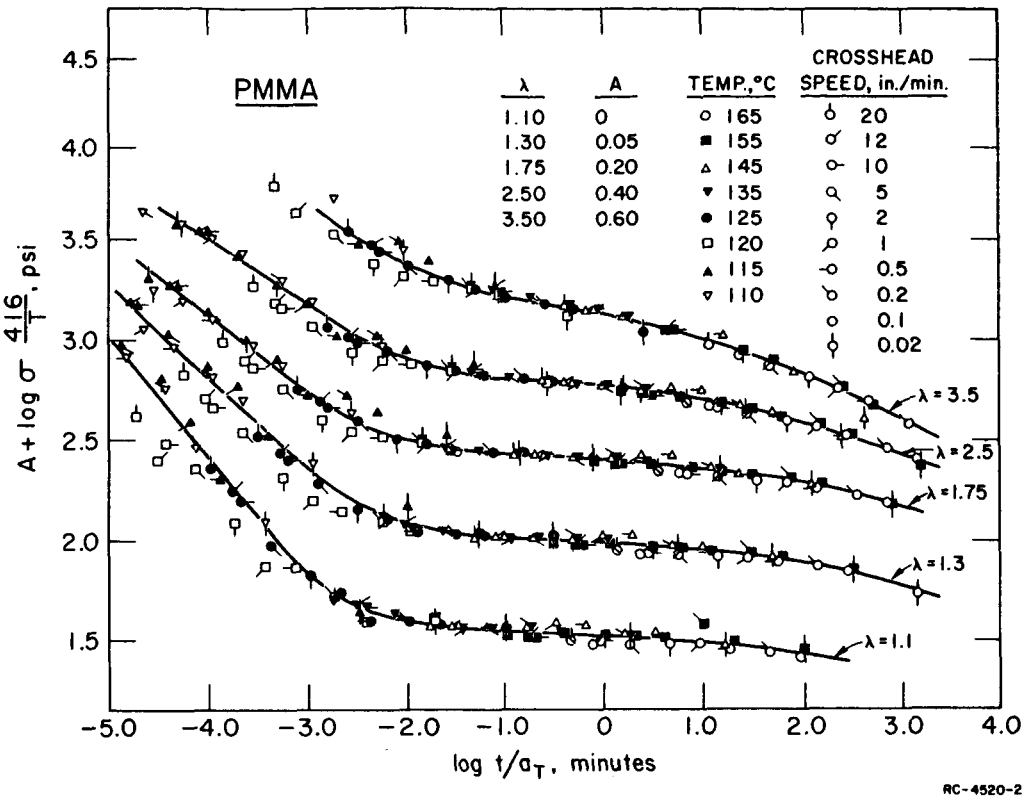

FIG. 2 VARIATION OF REDUCED STRESS WITH TIME AT DIFFERENT STRAIN VALUES OF UNCROSSLINKED PMMA. Temperature shift factors determined from Curve in Fig. 1

Over regions of time where the lines are parallel, the viscoelastic behavior may often be represented by the equation[1]

$$F(t) = g(\epsilon)\,\frac{\sigma(t)}{\epsilon}\,. \qquad (2)$$

Smith[1] has found that isochronal stress-strain data of elastomers are often linearized up to about 100% extension by letting $g(\epsilon)$ equal λ.

To test whether this would hold also for uncrosslinked PMMA, isochronal values of $\sigma\, T_s/T$ were read from graphs such as Fig. 2 and were plotted as reduced true stress, log $\lambda\sigma\, T_s/T$, against log $(\lambda-1)$ as shown in Fig. 3. An arbitrary additive constant A is again used to separate the curves.

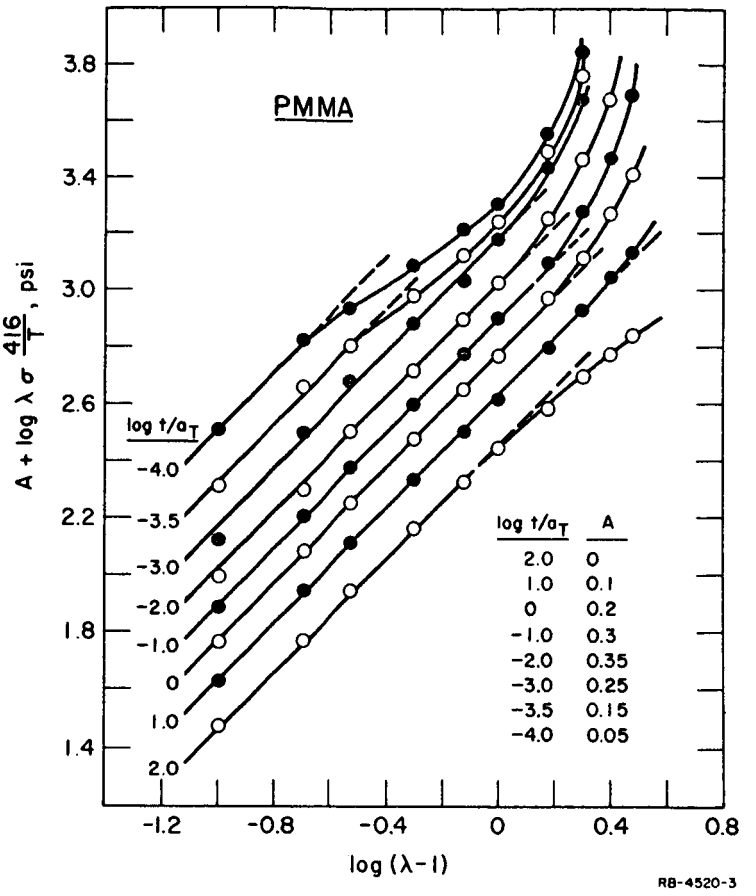

FIG. 3 ISOCHRONAL VALUES OF TRUE REDUCED STRESS AS A FUNCTION OF STRAIN FOR UNCROSSLINKED PMMA

Figure 3 shows that $g(\epsilon) = \lambda$ linearizes the plots up to about 100% extension ($\log (\lambda-1) = 0$) in the time region $0.001 < t < 100$ minutes. At shorter times significant departures from linearity become apparent. Since these short times correspond to temperatures near T_g (behavior in the rubber-to-glass transition zone) this is not surprising. An additional discussion of the curves will be given in the final report, after a more detailed and somewhat different analysis has been made of the experimental results.

In the final report a graph will also be shown of log F(t) vs. log t. This, as is apparent from Fig. 2, has an extended flat portion indicating a high entanglement coupling density. The modulus corresponding to the flat portion of log F(t) vs. log t is 340 psi, or 2.3×10^7 dynes/cm^2.

Figure 4 shows the failure envelope obtained by plotting log $\lambda_b \sigma_b T_s/T$ against log $(\lambda_b - 1)$ where the subscript b refers to values at break. Where

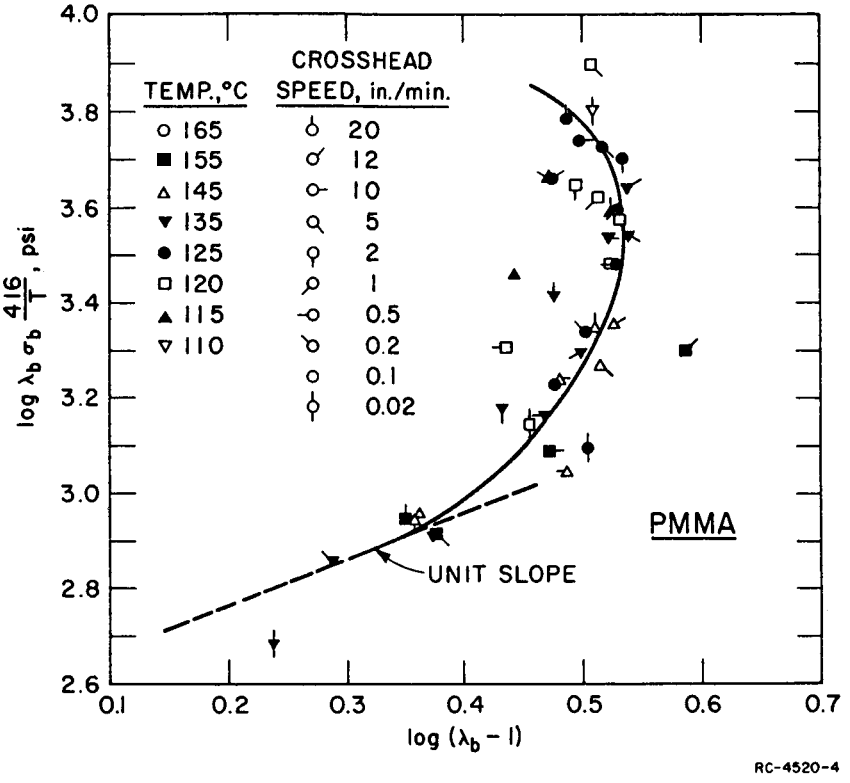

FIG. 4 FAILURE ENVELOPE FOR UNCROSSLINKED PMMA

the stress-time curves obtained on the Instron tester showed yield values (at lower temperatures and higher crosshead speeds) or contained an indication that flow had occurred during the extension (at higher temperatures and lower crosshead speeds), the break data were eliminated from the plot. However, these data were plotted in Fig. 5 and the corresponding temperature and crosshead speeds are tabulated below.

	Yield Region
Temperature °C	Crosshead Speed in./min.
110	20, 12, 10, 5, 2, 1, .5, .2, .1
115	20, 12, 10, 5, 2, 1, .5
120	20, 12, 10

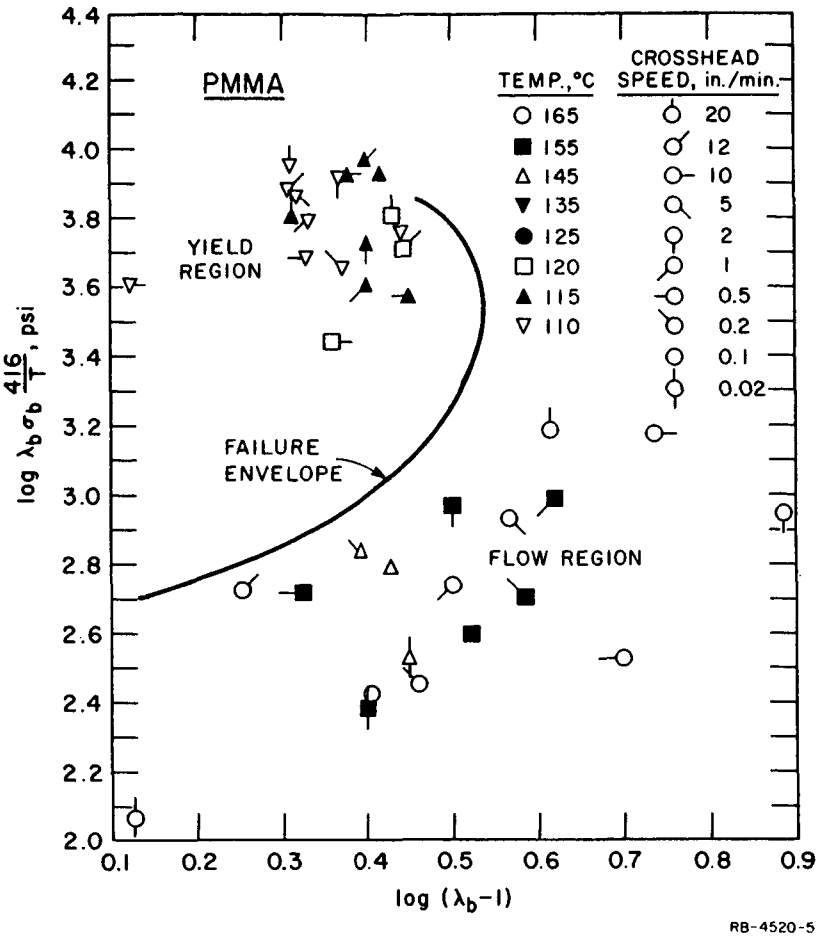

FIG. 5 YIELD REGION AND FLOW REGION OUTSIDE OF FAILURE ENVELOPE FOR UNCROSSLINKED PMMA

	Flow Region
Temperature °C	Crosshead Speed in./min.
145	.02, .1, .2
155	.02, .1, .2, .5, 1, 2
165	.02, .1, .2, .5, 1, 2, 5, 10, 12, 20

Hitherto failure envelopes had been obtained on crosslinked polymers only. Figure 4 demonstrates that the concept of the failure envelope is applicable also to uncrosslinked polymers, although a smaller segment of the envelope only is defined because of the occurrence of flow and yield. With crosslinked polymers the lower branch of the failure envelope asymptotically approaches the equilibrium stress-strain curve with increasing

temperature or decreasing crosshead speed. In this region the failure envelope (plotted logarithmically) has unit slope, and

$$\log \lambda\sigma = \log G_e \epsilon \tag{3}$$

where G_e is the equilibrium modulus. Uncrosslinked polymers do not have an equilibrium modulus, but if the entanglement coupling density is high, this results in a pseudo-equilibrium modulus indicated by a relatively flat portion of the constant strain rate modulus F(t), as mentioned above. In this case the lower branch of the failure envelope of an uncrosslinked polymer may also be expected to approach unit slope on a logarithmic plot. It is therefore interesting to note that the modulus obtained from the unit slope region of the envelope (even though it is not well defined because of the occurrence of flow) is 347 psi, in very good agreement with the modulus derived from the flat portion of F(t).

B. Crosslinked PMMA

Tensile tests were carried out on two samples of PMMA crosslinked with glycol dimethacrylate (GDMA). These samples were prepared at the Ames Research Center of NASA and contained 0.3 and 0.8 g of GDMA per 100 g of methylmethacrylate respectively. The number of moles of effective chains per unit volume, ν_e, of these samples is 0.359×10^{-4} and 0.953×10^{-4} respectively, calculated from

$$\nu_e = \frac{2x\rho}{M_A(100 + x)} \tag{4}$$

where x is the amount (in grams) of crosslinking agent added to 100 g of monomer, ρ is the density of the crosslinked material, and M_A(=198) is the molecular weight of the crosslinking agent.

Equation (4) was derived assuming 100% crosslinking efficiency which is justified at these relatively low crosslink densities.[6] The factor 2 enters because the number of effective chains per unit volume is equal to twice the number of crosslinking molecules.

Rings having outer diameters of 1.400 inches and inner diameters of about 1.27 inches were cut on a lathe from about 0.03-inch-thick sheets of the samples. The dimensions of the rings were obtained as described in the preceding report.

The rings were tested in the Instron tester at eight temperatures ranging from 110 to 165° C, and ten crosshead speeds, ranging from 0.02 to 20 inches/minute. Reduction and analysis of the data has not yet been completed. A detailed discussion of the results will be presented in the final report.

III STRESS RELAXATION

Continuous and intermittent stress relaxation measurements are being employed to study the degradation kinetics of the materials under investigation. Tests are to be conducted at elevated temperatures (from about 100 to 250° C), chiefly in vacuum, although air, inert gas, and controlled humidity atmospheres may also be employed. Some continuous stress relaxation data will be obtained in the rubber-to-glass transition region to characterize the viscoelastic properties of the materials.

The apparatus was designed to allow continuous and intermittent stress relaxation tests to be conducted simultaneously under identical test conditions. A number of technical difficulties, chiefly connected with the exacting temperature requirements, were encountered. These seem to have been successfully overcome for the most part, although there is still some problem in obtaining a uniform temperature distribution over the length of the specimen. The apparatus is currently being modified to eliminate the gradient.

A. General Description of Apparatus

A photograph of the apparatus is shown in Fig. 6. The stress relaxometer is built around a half-inch "main" brass support plate about two feet square, resting horizontally on a metal framework about five feet above ground. Mounted on top of the main plate are the vacuum pumping and monitoring apparatus, bath agitation motor, and a frame to guide, actuate, and set the extension on the connector rods. Mounted about three inches below and parallel to the main plate is a 10-inch round "vacuum" plate which receives a vertical inverted 8-inch bell jar (not shown in Fig. 6). The chamber thus formed houses a 6-inch round brass can which is also attached vertically to the vacuum plate, and contains the measuring stations. The front of the brass can is sliced-off, thereby exposing the stations to view.

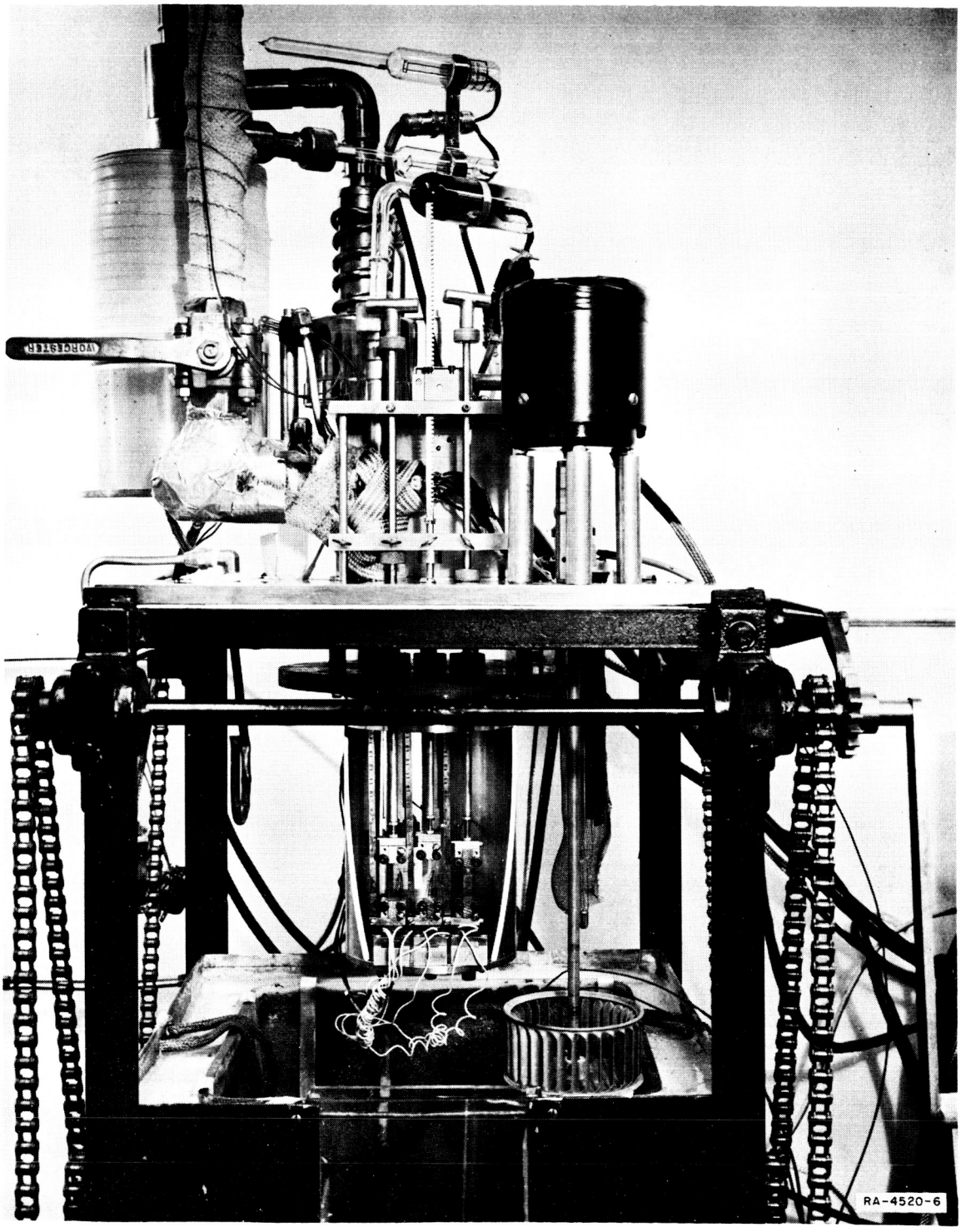

FIG. 6 STRESS RELAXOMETER

The temperature bath consists of a square Pyrex glass tank fitted inside a larger (2 foot square) metal tank, with insulation between the two. It is suspended on drive chains beneath the main plate and when raised to engage the top plate completely surrounds the test chamber. Rectangular glass windows in the front of the outside metal tank give a direct view of the stations and specimens when the bath is raised into operating position.

Three relaxometer stations are used. The center station serves to set the desired strain, and to get a preliminary indication of the magnitude of the forces that will be experienced in the other two active stations. In each station, the specimen is mounted vertically between two clamps, and is extended by pulling the top clamp upward by means of a connecting rod, which is sealed by O-rings, through the vacuum plate and main plate. The bottom clamp, which remains essentially fixed, is attached to the tip of a cantilever beam load cell. The beam is clamped parallel to the bottom of the brass housing can. The rods connecting to the top clamps are threaded on the portion extending above the main plate and are fitted with knurled nuts positioned between the main plate and a brass "datum" bar. The rods pass through this horizontal bar and are held in vertical alignment by passing through a horizontal frame about 10 inches above the main plate.

The datum bar travels on guides vertical to the main plate and is used to set the strain on the two active test stations to the left and right. In practice, the datum bar is fixed at a particular height above the main plate as dictated by the preliminary extension on the center station. The knurled nuts on each of the rods connecting to the test stations are screwed down to the main plate, and the rods are pulled up; the rod travel (and therefore sample extension) is positively stopped when the nut on the connecting rod reaches the now-fixed datum bar. Pre-set, nearly identical strains can be obtained on each of the 2 active test specimens. All connections are rigid and alignment of the test specimen along the axis of pull are fixed and perfect, preventing sideways distortion of the sample.

B. Temperature Control and Monitoring

The apparatus was designed so that either oil or air can be used as a bath medium. When air is used, two 250-watt finned heat exchangers are placed at the bottom of the glass bath tank as shown in Fig. 6. A blower type impeller is then used to circulate the air. When oil is used, two 500-watt stainless steel immersion heaters are inserted through holes in the main plate and the bath is stirred by a propeller type agitator. Either agitator is driven from a motor located on top of the main plate. Each of the heaters is governed by individual autotransformers. One of the heaters is run continuously at a power level yielding ~90% of test temperature. The other (at 10%) is used as a control heater. The control heater is governed by a Lux Model L151 mercury control relay, which in turn is governed by Lux Model L150/3 immersion type mercury sensor. This shunts part of the current through the relay when the desired upper temperature limit is reached. The control relay is thereby deactivated and the control heater cut off.

Ten copper-constantan thermocouples are used to measure the temperature at various points in the system; seven are contained within the vacuum chamber utilizing a common constantan leg and reference junction. The reference junction is maintained at 0^{o} C in a ice slush bath. The remaining three thermocouples are used to measure temperatures at various points in the bath. The thermocouple emf's are read on a standard Rubicon laboratory potentiometer with a resolution of ±0.001 mV.

The thermocouples were calibrated *in situ* against a platinum-platinum-10% rhodium secondary standard thermocouple in a copper block with all reference junctions in the same ice slush bath at 0^{o} C.

C. Vacuum Pumping and Gaging Equipment

A Welch Model 5-71740 mechanical fore pump, CEC Model VFM 10 oil diffusion pump, and a cold trap are used for vacuum pumping. Maximum pumping speed at 0.1μ is 600 liters/minute. Maximum blanked-off pressure is 1.0×10^{-6} mm Hg (according to manufacturer's specifications).

The actual ultimate vacuum achieved with a cold, empty system was 5.0×10^{-6} mm Hg.

A Pirani gauge monitors the vacuum in the range 1-20μ Hg, and a hot-cathode ionization gage below 1μ, the main area of interest. The standard VG1A ionization tube, rated at 100 μA/micron at 5 mA emission in air, is used, with emission regulated at ±1% at 5 mA.

D. Load Cells

The friction problem encountered when a load cell is placed outside a sealed system and connected into the system by rods, diaphragms, etc., has been avoided by placing the load cells within the vacuum system. The severe temperature requirements generated special problems concerning choice of materials and stability.

Only inorganic materials were used in the construction of the load cells to maintain a clean vacuum. Thus far they have sustained many cycles to 250° C with no detectable change in basic properties.

The bottom clamp of each relaxometer station is rigidly fixed perpendicular to the tip of a cantilever-beam load cell which is clamped like a diving board parallel to the bottom of the relaxometer housing.

Two Microdot Inc. SG101-A-1 dual 120Ω resistance strain gages are welded to the stainless steel beam; one each on the top and bottom surfaces near the clamp where maximum stress occurs when the beam is bent in this configuration.

The strain gages occupy two adjacent active arms of a classical resistive Wheatstone bridge, utilizing a 10 volt D.C. excitation. The small changes in the resistance of the strain gages upon bending of the beam are shown as linearly proportional voltage differences. After appropriate calibration with dead weights, the voltage difference on the bridge is interpreted as a direct linear indication of force on the test specimen.

The electrical output (voltage difference) from a resistive-bridge load cell of this type is determined by the following linear relationship:

$$E_o = \frac{1}{4} GnE_{ex}\epsilon \qquad (4)$$

where E_o is the output from the bridge in microvolts, G is the gage factor of the strain gages, n the number of active gages (2), E the bridge excitation voltage in volts, and ϵ the mean strain on the gages over the length of the gage (x 10^6). The gage factor is given by $\Delta R/R\epsilon$, and is ~1.55 in this case.

The strain gages are temperature-compensated, i.e., they are heat treated to achieve a negative resistance/temperature slope so that when mounted on the steel beams, the error caused by thermal expansion of the beam, which would appear as an erroneous indication of loading, is minimized. The temperature slope of the gage is adjusted according to the coefficient of thermal expansion of the particular steel used (in this case 17-4 PH stainless steel with a strain of 6 ppm/^oC). Temperature stability of the load cell is further improved by the relative positions of the strain gages in adjacent arms of the bridge where spurious outputs are subtractive and tend to cancel. The Wheatstone bridge "completion resistors" (so called because they are inactive "dummies," serving no purpose other than to complete the necessary 4 resistors of the bridge), are located outside the test apparatus at room temperature. A spurious change in the resistance of these resistors, or in the wires connecting them with the load cell in the test apparatus, would also be a source of error. Carefully matched, stress-relieved, wirewound, precision manganin resistors were chosen to minimize this source of error. They have a small resistance/temperature slope at room temperature (24-27^o C) of less than 15 ppm as determined in an actual test on an ESI system. Again, since the completion resistors and connecting wires are in adjacent arms of the bridge, this type of error is further attenuated by the fact that similar resistance changes will be subtractive.

Preliminary in situ tests encompassing all temperature effects indicated a temperature sensitivity of less than 4 $\mu V/^{o}C$ maximum (at 10 V excitatation) over the range of ambient temperature to 250° C. Also, adjustment of the resistance/temperature slope of the strain gages by heat treatment yields a null at about 150° C, which means that most of our tests will occur in relatively flat portions of the output vs. temperature curve, where $\Delta E_o/\Delta t$ will probably be considerably less than the maximum. Moreover, the cumulative output can be zeroed out, using a balancing circuit, just prior to the initiation of a test. Since temperature variation in the chamber during the actual test period is to be held to less than 0.5° C, thermal drift in the output of the load cells is insignificant at the design output levels.

The sensitivity of the load cell--its gage factor or its electrical output versus load--changes as a linear function of temperature by 0.0 18%/°C. This error is taken into account in the calculation of the stress. Reproducibility of the load cells is better than 1% over 100 or more cycles of loading, and creep is virtually undetectable at the design loads.

The load cell outputs are read on a Beckman Instruments Type RS, two-channel Offner Dynagraph with high impedance (500 KΩ input minimum) solid state chopper amplifiers. Frequency response is 10% up to 200 cps; full 7 cm galvanometer deflection time is 2.5 milliseconds. Internal calibration is provided and load cell calibration is effected in situ against this internal calibration provision, providing independence from periodic calibrations against outside standards. Noise-free sensitivities as high as 50 μV/cm are provided with over 300 cm of zero suppression available (relative to the 7 cm full scale deflection). The long term gain stability is 0.5% and the short term drift 1 μV/hour. Available paper speeds are 1, 5, 25, and 125 mm/sec. Lineraity is 0.5%.

Excitation for the load cell bridges is provided by Endevco Model SR-200 EP solid state regulated power supplies. Regulation was found to be better than 0.1% by actual test. Long term or thermal drift was virtually

undetectable at 0.01% resolution over 48 hours. Originally the excitation provisions of the strain gage coupler on the Offner Dynagraph were used, but they were abandoned because they were not stable enough.

Balancing (zeroing) of the load cell circuit just at the beginning of a test is accomplished by means of two potentiometers placed in parallel with the bridge, with their center taps connected to the positive output from the bridge. One is used for coarse adjustment (20 KΩ) and the other for fine adjustment (a variable 10 KΩ potentiometer between two 500 KΩ fixed resistors). The over-all resistance of one side of the bridge is adjusted with these parallel resistances to match the other half--resulting in a balanced bridge and zero output.

The present set of load cells were designed with a sensitivity of ~0.4 mV/kg. For the loads encountered when testing PMMA samples (cross sectional area: ~0.05 cm^2) in the glassy or the transition region, they are perfect, permitting a system precision of much better than 1%. However, in the rubbery region where loads as low as 0.1 kg (maximum) are encountered, the outputs from the load cells (e.g., 0.04 mV at 0.1 kg.) do not permit the desired precision. The readout resolution is about ±0.002 mV. In a typical relaxation curve in the rubbery region, where the force relaxes to a small percentage of the maximum within a few seconds, the currently available precision must be improved. Accordingly, a second set of load cells is being assembled with about 50 times the sensitivity of the first. This is for use in the rubbery region. The load cells will be identical to the first set in all respects except that the stainless steel beam will be thinner to increase the sensitivity.

E. Strain Determination

The strain on the sample is determined by direct observation of bench marks on the specimen from outside the apparatus using an upright cathetometer with a resolution of ±0.005 cm.

As mentioned earlier, the apparatus is designed to achieve pre-set identical strains in both test stations. In practice the strains are

not quite identical. This is probably due to the unavoidable extension of the samples from the sample holders, which occurs to different extents.

F. Experimental Work

To check the temperature distribution inside the vacuum chamber, 1 x 0.25 x 0.03 inch specimens of uncrosslinked commercial PMMA were placed between the clamps in the left station. Thermocouples were inserted in the holes provided in the clamps for this purpose, and in three holes drilled in the middle and at the two ends of the specimen near the clamps. The temperature was raised to about 115-120° C (using the air bath) and the temperature registered by the thermocouples were recorded. The procedure was then repeated pumping down to about 20 microns of vacuum. The experiments were carried out in the left station only because of the limited number of thermocouples available inside the vacuum chamber. However, previous tests had shown that there was very little difference between the clamp temperatures of the left and right stations, undoubtedly due to the high degree of symmetry in the apparatus with respect to these two stations.

These measurements indicated the existence of a negative temperature gradient from the middle of the specimen outward towards its ends. The heat drain appears to be due to conduction through the brass connecting rods (upper clamp) and the brass housing can (lower clamp). Since the lower clamp is partially insulated from the housing can by the stainless steel beams which are poorer heat conductors, the drain from the lower is less than that from the upper clamp.

A method of insulation by reducing the thermal paths to point contacts is currently being implemented and will be reported on in the next report.

To test the over-all performance of the apparatus, specimens similar to those described above were inserted in all three stations and were given extensions of about 10% in about 5 microns of vacuum at a temperature of about 115° C. The stress relaxation curves calculated from the

data obtained in both the left (No. 1) and the right (No. 2) station are plotted in Fig. 7. There is excellent agreement between the two

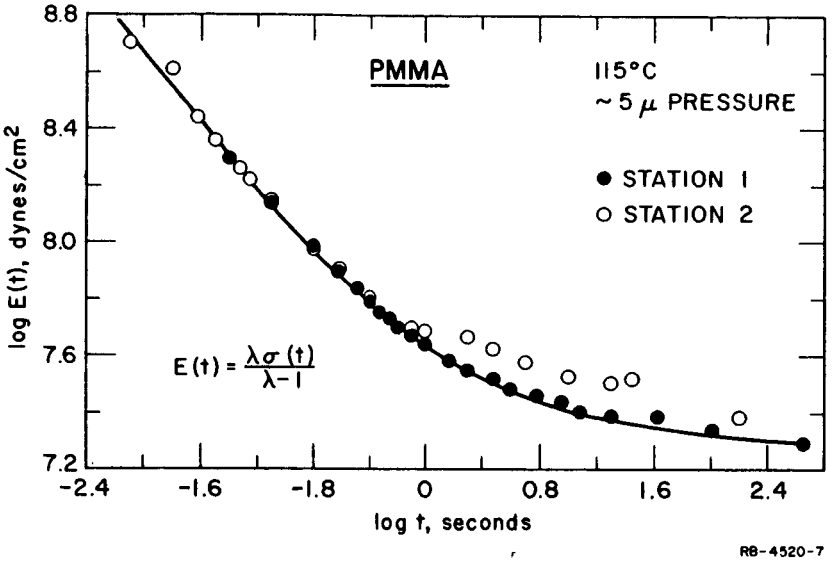

FIG. 7 STRESS RELAXATION CURVE OBTAINED IN TEST OF UNCROSSLINKED PMMA

stations except at long times where the No. 2 values lie above the curve. This is explained by the fact that half of the active bridge in this station had become inoperative prior to the test. In consequence, the gage became poorly balanced thermally and the sensitivity was reduced to about 0.2 μV/kg resulting in poorer readings at longer times. The curve is in substantial agreement with published results by Tobolsky[7] and Fujino et al.[8] It should be noted that apparently quite satisfactory results could be obtained in this apparatus at times as short as 0.01 second.

REFERENCES

1. Smith, T. L., Trans. Soc. Rheology 6, (1962).

2. Smith, T. L., J. Polymer Sci. 1A, 3597 (1963).

3. Smith, T. L., J. Appl. Phys. 35, 27 (1964).

4. Smith, T. L., Proceedings of the Fourth International Congress on Rheology (in press).

5. Ferry, J. D., "Viscoelastic Properties of Polymers," John Wiley, New York, 1961, Chapter II-5.

6. Loshaek, S., and T. G. Fox, J. Am. Chem. Soc. 75, 3544 (1953).

7. Tobolsky, A. V., "Properties and Structure of Polymers," John Wiley, New York, 1960, Chapter V.

8. Fujino, K., K. Senshu, and H. Kawai, J. Colloid Sci., 16, 262 (1961).